

Periodic self-accelerating beams by combined phase and amplitude modulation in the Fourier space

Yi Hu,^{1,2,*} Domenico Bongiovanni,¹ Zhigang Chen,^{2,3} and Roberto Morandotti¹

¹INRS-EMT, 1650 Blvd. Lionel-Boulet, Varennes, Québec J3X 1S2, Canada

²The MOE Key Laboratory of Weak Light Nonlinear Photonics, School of Physics and TEDA Applied Physics School, Nankai University, Tianjin 300457, China

³Department of Physics & Astronomy, San Francisco State University, San Francisco, California 94132, USA

*Corresponding author: hynankai@gmail.com

Received May 3, 2013; revised July 31, 2013; accepted August 1, 2013;
posted August 7, 2013 (Doc. ID 189976); published August 26, 2013

We propose and demonstrate the generation of periodic self-accelerating beams through both phase and amplitude modulation in the Fourier space. For small amplitude variations, an accelerating beam still follows a smooth convex trajectory, which can be traced by acting on the spectral phase only. However, large modulations such as those generated from the Heaviside function with a zero amplitude distribution partially modify the convex trajectory due to the appearance of straight-line paths. Furthermore, periodic self-accelerating beams along convex trajectories are realized by employing an array of “spectral wells” in both the paraxial and nonparaxial regimes. © 2013 Optical Society of America

OCIS codes: (070.7345) Wave propagation; (070.4790) Spectrum analysis; (050.1970) Diffractive optics.
<http://dx.doi.org/10.1364/OL.38.003387>

Curved or self-accelerating light beams have recently received a great deal of attention, triggered by the introduction of nondiffracting Airy beams capable of traveling along a parabolic trajectory [1–3]. Driven by fundamental interest as well as potential applications, the judicious design of self-accelerating beams has been expanded from the initial realization of a simple parabolic trajectory to the generation of an arbitrary convex trajectory, through phase engineering in both the real and Fourier spaces and under both paraxial and nonparaxial conditions [4–13]. Very recently, accelerating beams along periodic rather than smooth trajectories have also been proposed [9] and observed [8,14] in the nonparaxial regime. The realization of such “zigzag” or “snake-like” optical beams through different approaches [15–17] is of particular interest for a variety of applications.

In this Letter, we generate periodic self-accelerating beams by engineering the spectrum of a light beam. As mentioned before, such beams have been realized by applying both spectral phase and amplitude modulations in the nonparaxial case [8,14], but here we give a general and detailed explanation on these beams in both paraxial and nonparaxial conditions via a spectral language, hence leading to a method to engineer periodic accelerating beams by merely rearranging the straight-line propagations.

In the paraxial limit, the spectral evolution of a coherent monochromatic light along the z axis can be described as

$$\tilde{E}(k_x, z) = A(k_x) \exp[-ik_x^2 z / (2k) + i\rho(k_x)], \quad (1)$$

where $A(k_x) \geq 0$ is the spectral amplitude, k_x is the transverse wave number, k is the vacuum wave number, and $\rho(k_x)$ is an imposed smooth phase in the spectral domain. In our previous work [7] on the generation of self-accelerating beams through Fourier-space phase engineering, $A(k_x)$ is assumed to be a unit constant. Then, the spatial variable can be described as

$$x = k_x z / k - \rho'(k_x), \quad (2)$$

where x is the position in the real space, while the superscript $'$ represents the first derivative with respect to k_x . From Eq. (2) we can infer that the spectral density $D(k_x) = dk_x / dx$ is, within a small area dx , equal to $1/|\mu''(k_x)|$, where $\mu(k_x) = -k_x^2 z / (2k) + \rho(k_x)$, as seen from Eq. (1). Consequently, a spectrum-to-distance mapping can be realized when the spectral density becomes singular, i.e.,

$$\mu''(k_x) = -z/k + \rho''(k_x) = 0, \quad (3)$$

from which one can find a specific key frequency that is mapped into the propagation distance, leading to the possibility of transforming a spectral fluctuation into a longitudinal oscillation associated with an accelerating beam [7]. By solving Eqs. (2) and (3), the trajectory of a self-accelerating beam with a homogeneous spectral amplitude can thus be obtained. However, when $A(k_x)$ is not a constant in Eq. (1), the above analysis needs to be revisited. Since the weight of each frequency component is no longer uniform, the spectral density $D(k_x)$ takes the new form of $A(k_x)/|\mu''(k_x)|$. Provided that the spectral amplitude is larger than zero, i.e., $A(k_x) > 0$, and the amplitude variation is small, the analysis related to Eq. (3) is still valid. We note, however, that this approach would not work when $A(k_x)$ is 0 for certain values of k_x . To study the influence of amplitude modulations on self-accelerating beams, we start from the simplest case—a Heaviside-shaped spectrum, i.e.,

$$A(k_x) = \begin{cases} 1 & k_x \leq k_{x0} \\ 0 & k_x > k_{x0} \end{cases}. \quad (4)$$

We still assume $\rho''(k_x)$ to be a monotonically increasing function of k_x , which results in a single convex trajectory [schematically shown by the solid line in Fig. 1(a)] for the self-accelerating beams under test [7]. For $A(k_x) = 1$,

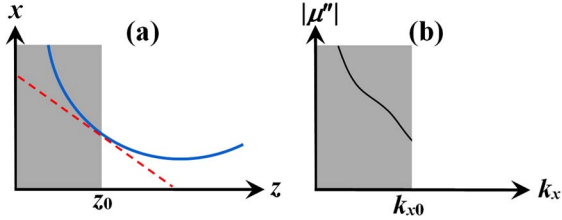


Fig. 1. (a) Schematics of the beam path composed of straight and convex lines and (b) $|\mu''|$ related to a Heaviside-spectral distribution.

Eq. (3) can be still used to determine the trajectory in the range $z \leq z_0 = k\rho''(k_{x0})$. However, at $z > z_0$, the beam path cannot be described by the curved trajectory any more. For these distances, the spectrum density approaches the maximum only when $|\mu''(k_x)|$ is the minimum at $k_x \leq k_{x0}$. Considering that $\rho''(k_x)$ increases monotonically, $\mu''(k_x)$ is always less than 0 and it also increases monotonically for any $z > z_0$. $|\mu''(k_x)|$ is schematically plotted in Fig. 1(b). Therefore, the spectrum density reaches the maximum only at the discontinuity point k_{x0} , for a distance $z > z_0$, where the key frequency is (always) k_{x0} . Accordingly, the beam path at $z > z_0$ can be traced via Eq. (2):

$$x = k_{x0}z/k - \rho'(k_{x0}). \quad (5)$$

Equation (5) is linear with distance, as schematically shown by the dashed red line in Fig. 1(a). From Eqs. (2)–(5), one can readily infer that the straight line is tangent to the curved trajectory at the tangent point $z = z_0$ [18]. Thus, the curved and straight lines join together to form the trajectory of an accelerating beam provided that its spectral amplitude has a Heaviside shape. Consequently, the beam follows a curved path at $z < z_0$ and a straight path elsewhere. We mention that even if the spectral distribution is not zero at $z > z_0$, e.g., by adding a constant on Eq. (4), the generated self-accelerating beam still follows the same path, since the new amplitude modulation manifests an equivalent feature as does the Heaviside-shaped spectral distribution. Similar results can be obtained with $\rho''(k_x)$ being monotonically decreasing with respect to k_x .

In order to corroborate the argument above, let us discuss a typical spectral phase modulation: the cubic function $\rho(k_x) = [a(k_x - b)/k]^3$ (where $a^3 = -4 \times 10^6$, $b = 0.033k$) [19]. Without an appropriate amplitude modulation, the beam follows the parabolic trajectory $kz^2/(12a^3) + bz/k$, as shown in Fig. 2(a). However, in the presence of a spectral Heaviside distribution (here k_{x0} is $-0.005k$), as expressed by Eq. (4), the beam follows the parabolic curve only up to $z = z_0 = 6a^3(k_{x0} - b)/k^2$ but then turns into a straight line at $z > z_0$. The beam evolution calculated from Eq. (1) further confirms our analytical predictions. For the portion related to straight-line propagation, the beamwidth of the main lobe increases dramatically [Fig. 2(b)]. By discarding the sublobes, the residual spectra corresponding to the main lobe of the beam in Fig. 2(b) are plotted in Fig. 2(c), well matching the analytic results.

We now present the corresponding experimental results, obtained using a setup similar to the one employed

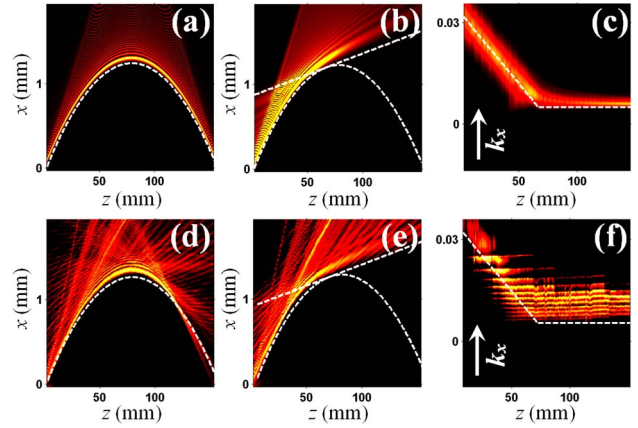


Fig. 2. Numerical simulations (first row) and experimental observations (second row) of Airy beams generated (a), (d) without and (b), (e) with a Heaviside-shaped amplitude modulation. (c), (f) Spectral components related to the main lobes in (b) and (e), respectively. The dashed white lines/curves in (a)–(c) are calculated from theory.

in our previous work [7]. A spatial phase modulator (SLM) is placed at the front focal plane of a cylindrical lens ($f = 100$ mm) in order to achieve a suitable phase modulation for the broad beam ($\lambda = 633$ nm), while a camera is employed to monitor the evolution of the planar beam behind the lens. An amplitude mask (a structure printed on a transparent paper) is tightly positioned close to the SLM to create the desired intensity distribution for the input beam. Our experimental observations, shown in Figs. 2(d)–2(f)—where each scanned beam is averaged—are in good agreement with the numerical results presented in Figs. 2(a)–2(c).

Next, let us extend the previous analysis to more general cases. One straightforward extension consists in modulating the amplitude through a spectral “well”, i.e., $A = 0$ for $k_{x1} \leq k_x \leq k_{x2}$ and $A = 1$ elsewhere, as shown in Fig. 3(a). By imposing such an amplitude

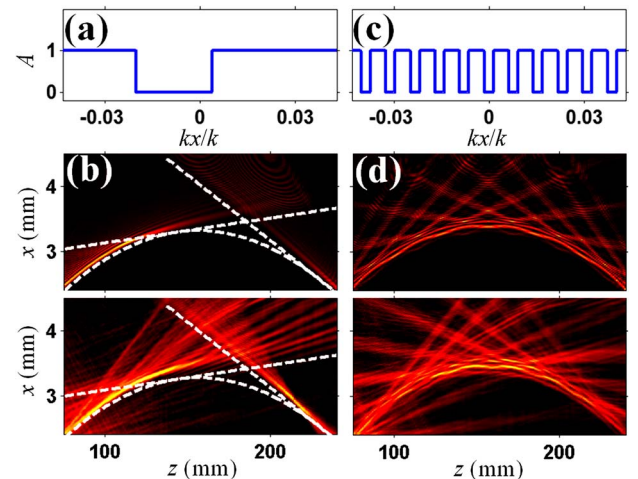


Fig. 3. Generation of periodic accelerating beams along a parabolic curve by employing (a), (b) one spectral well and (c), (d) an array of spectral wells. (a), (c) k -space amplitude modulation relative to the results in (b) and (d), where the upper and bottom panels correspond to numerical and experimental results, respectively.

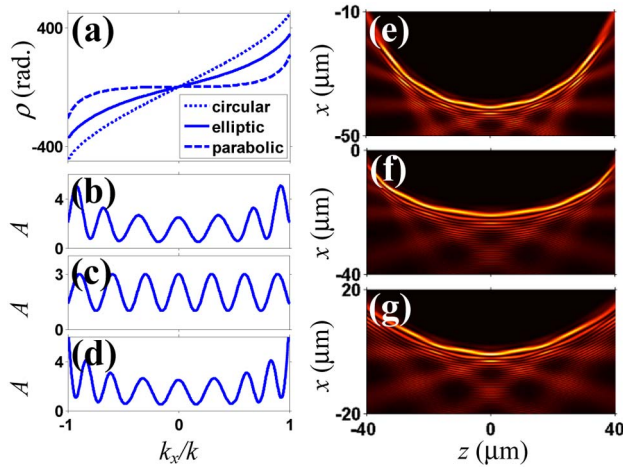


Fig. 4. Nonparaxial periodic self-accelerating beams. (a) Imposed phases and (b)–(d) amplitude modulations employed for generating periodic accelerating beams along (e)–(g) circular, elliptic, and parabolic trajectories, respectively.

modulation combined with a typical cubic phase modulation $[a(k_x - b)/k]^3$ (where $a^3 = -6 \times 10^6$, $b = 0.043k$), the beam trajectory thus generated is composed of two straight lines in the range $6a^3(k_{x2} - b)/k^2 < z < 6a^3(k_{x1} - b)/k^2$ and of a parabolic curve elsewhere, as confirmed by both our simulations and the experimental results shown in Fig. 3(b). In fact, for any imposed phase $\rho(k_x)$ with its second derivative being a monotonic function, the area Δz confined by $z_1 = k\rho''(k_{x1})$ and $z_2 = k\rho''(k_{x2})$ is positively correlated to $\Delta k_x = |k_{x2} - k_{x1}|$. Provided that Δk_x is small enough for a given $\rho''(k_x)$, the “V” shape formed by the two straight lines approaches the parabolic curve asymptotically. In this way, the spectral well does not cause a severe distortion to the convex trajectory of the generated self-accelerating beam.

Furthermore, one can envision that the “V”-shaped path may be exploited as an ingredient for constructing a periodically wiggling beam by using cascaded spectral wells. As a typical example, we employ a periodic amplitude modulation superimposed to the same cubic phase, as depicted in Fig. 3(c). Corresponding numerical and experimental results are shown in Fig. 3(d). As expected, the main lobe of the beam follows a zigzag rather than a smooth convex trajectory, yet accelerating as the conventional Airy beam does, with the zigzags matched by a series of “V”-shaped straight lines as described in Eq. (5). Similar to the characteristic feature of a “V”-shaped path, if the width for each spectral well is not large enough, the oscillation of the main lobe becomes weak or may even disappear.

In the nonparaxial regime, the previous analysis is still applicable. Some typical results are shown in Fig. 4.

Our scheme is able to explain, via the spectral language, the results observed in the nonparaxial case [8,14], where both spectral phase and amplitude were employed. By using a spectrum-to-distance mapping, it is straightforward to engineer periodic accelerating beams that can have reduced side lobes as desired [20].

In conclusion, we have studied the combined effect of spectral phase and amplitude modulations on the

dynamics of self-accelerating beams. We found that, while the beam path still follows the convex trajectory induced only by a suitable spectral phase at small amplitude modulations [20], large spectral modulations such as those from the Heaviside distribution partially modify the convex trajectory. In particular, the proposed periodic accelerating beams are realized through an array of spectral structures in the paraxial limit experimentally and in the nonparaxial regime numerically.

This work is supported by the Natural Sciences and Engineering Research Council of Canada (NSERC), via the Discovery and Strategic grant programs, and by the U.S. National Science Foundation and AFOSR funding agencies.

References

1. G. A. Siviloglou and D. N. Christodoulides, *Opt. Lett.* **32**, 979 (2007).
2. G. A. Siviloglou, J. Broky, A. Dogariu, and D. N. Christodoulides, *Phys. Rev. Lett.* **99**, 213901 (2007).
3. Y. Hu, G. Siviloglou, P. Zhang, N. Efremidis, D. Christodoulides, and Z. Chen, in *Nonlinear Photonics and Novel Optical Phenomena*, Z. Chen and R. Morandotti, eds. (Springer, 2012), Vol. **170**, pp. 1–46.
4. E. Greenfield, M. Segev, W. Walasik, and O. Raz, *Phys. Rev. Lett.* **106**, 213902 (2011).
5. L. Froehly, F. Courvoisier, A. Mathis, M. Jacquot, L. Furfaro, R. Giust, P. A. Lacourt, and J. M. Dudley, *Opt. Express* **19**, 16455 (2011).
6. I. D. Chremmos, Z. Chen, D. N. Christodoulides, and N. K. Efremidis, *Phys. Rev. A* **85**, 023828 (2012).
7. Y. Hu, D. Bongiovanni, Z. Chen, and R. Morandotti, “Multi-path multi-component self-accelerating beams through spectrum-engineered position mapping,” arXiv: 1307.0891 (2013).
8. A. Mathis, F. Courvoisier, R. Giust, L. Furfaro, M. Jacquot, L. Froehly, and J. M. Dudley, *Opt. Lett.* **38**, 2218 (2013).
9. I. Kaminer, R. Bekenstein, J. Nemirovsky, and M. Segev, *Phys. Rev. Lett.* **108**, 163901 (2012).
10. F. Courvoisier, A. Mathis, L. Froehly, R. Giust, L. Furfaro, P. A. Lacourt, M. Jacquot, and J. M. Dudley, *Opt. Lett.* **37**, 1736 (2012).
11. P. Zhang, Y. Hu, D. Cannan, A. Salandrino, T. Li, R. Morandotti, X. Zhang, and Z. Chen, *Opt. Lett.* **37**, 2820 (2012).
12. P. Zhang, Y. Hu, T. Li, D. Cannan, X. Yin, R. Morandotti, Z. Chen, and X. Zhang, *Phys. Rev. Lett.* **109**, 193901 (2012).
13. P. Aleahmad, M. Miri, M. S. Mills, I. Kaminer, M. Segev, and D. N. Christodoulides, *Phys. Rev. Lett.* **109**, 203902 (2012).
14. E. Greenfield, I. Kaminer, and M. Segev, in *Frontiers in Optics Conference*, OSA Technical Digest (online) (Optical Society of America, 2012), paper FW1A.2.
15. J. Morris, T. Cizmar, H. Dalgarno, R. Marchington, F. Gunn-Moore, and K. Dholakia, *J. Opt.* **12**, 124002 (2010).
16. J. Zhao, P. Zhang, D. Deng, J. Liu, Y. Gao, I. D. Chremmos, N. K. Efremidis, D. N. Christodoulides, and Z. Chen, *Opt. Lett.* **38**, 498 (2013).
17. J. Rosen and A. Yariv, *Opt. Lett.* **20**, 2042 (1995).
18. J. D. Ring, C. J. Howls, and M. R. Dennis, *Opt. Lett.* **38**, 1639 (2013).
19. Y. Hu, P. Zhang, C. Lou, S. Huang, J. Xu, and Z. Chen, *Opt. Lett.* **35**, 2260 (2010).
20. S. Barwick, *Opt. Lett.* **36**, 2827 (2011).